IDENTIFICATION OF AN EARLY SUBSET OF CEREBELLAR NUCLEI NEURONS IN MICE

Maryam Rahimi-Balaei[1,2], Shayan Amiri[1,3], Thomas Lamonerie[4], Sih-Rong Wu[5,6,7], Huda Y. Zoghbi[6,7,8], G. Giacomo Consalez[9,10], Daniel Goldowitz[2], and Hassan Marzban[1,*]

[1]Department of Human Anatomy and Cell Science, The Children's Hospital Research Institute of Manitoba (CHRIM), Max Rady College of Medicine, Rady Faculty of Health Sciences, University of Manitoba, Winnipeg, Manitoba, Canada

[2]Department of Medical Genetics, Centre for Molecular Medicine and Therapeutics, BC Children's Hospital Research Institute, University of British Columbia, Vancouver, BC, Canada

[3]Department of Pharmacology and Therapeutics, Division of Neurodegenerative Disorders, St Boniface Hospital Albrechtsen Research Centre, University of Manitoba, Winnipeg, MB, Canada

[4]Université Côte d'Azur, CNRS, Inserm, iBV, France

[5]University of California San Francisco (UCSF), San Francisco, California, USA

[6]Department of Neuroscience, Baylor College of Medicine, Houston, TX, 77030, USA

[7]Jan and Dan Duncan Neurological Research Institute at Texas Children's Hospital, Houston, TX, 77030, USA

[8]Howard Hughes Medical Institute, Baylor College of Medicine, Houston, TX, 77030, USA

[9]Division of Neuroscience, IRCCS Ospedale san Raffaele

[10]Università Vita-Salute San Raffaele, 20132 Milan, Italy

Address correspondence to: Dr. H. Marzban, Department of Human Anatomy & Cell Science, Rm 129 BMSB, 745 Bannatyne Avenue, Max Rady College of Medicine, Rady Faculty of Health Sciences, University of Manitoba, Winnipeg, Manitoba, R3E 0J9, Canada

Tel: 204-789-3467

Fax: 204-789-3920

Email: hassan.marzban@umanitoba.ca

Manuscript: 29 Pages; 9 Figures; 0 Tables

Key Words: Cerebellar nuclei, SNCA, MEIS2, OTX2, Atoh1

Running Title: Rostroventral subset of cerebellar nuclei neurons

ABSTRACT

Cerebellar nuclei (CN) neurons serve as the primary output of the cerebellum and originate from the cerebellar primordium at early stages of cerebellar development. Employing various methodologies, we have characterized a specific subset of CN neurons that do not originate from the rhombic lip or ventricular zone of the cerebellar primordium. Embryos were collected at early stages of development and processed for immunohistochemistry (IHC), Western blotting, *in situ* hybridization (ISH), embryonic culture, DiI labeling, and flow cytometry analysis (FCM). Our findings indicate that a subset of CN neurons expressing α-synuclein (SNCA), OTX2, MEIS2, and p75NTR (NGFR) are located in the rostro-ventral (rv) region of the nuclear transitory zone (NTZ), while CN neurons derived from the rhombic lip are positioned in the caudo-dorsal (cd) area of the NTZ in the cerebellar primordium. Utilizing Otx2-GFP and Atoh1$^{-/-}$ mice, we have determined that these cells do not originate from the germinal zone of the cerebellar primordium. These results suggest the existence of a novel extrinsic germinal zone for the cerebellar primordium, possibly the mesencephalon, from which early CN neurons originate.

SIGNIFICANCE STATEMENT

The cerebellum contains a variety of distinct neuronal populations, each playing a significant role in its function within the brain. This research demonstrates that a particular subset of cerebellar nuclei neurons originates from a previously unrecognized germinal zone specific to the cerebellar primordium, independently of Atoh1's influence.

INTRODUCTION

In the mouse, the cerebellar primordium emerges at approximately embryonic day (E) 7–E8 as a neuroepithelial swelling on the rostral lip of the fourth ventricle, which is part of the alar plate of the metencephalon (rhombomere-1) (Kebschull et al., 2023, Goldowitz and Hamre, 1998, Sotelo, 2004, Wang and Zoghbi, 2001a, Marzban et al., 2015). The cerebellar primordium is rostrally limited by the isthmus, the mesencephalon-rhombencephalon (rhombomere-1, r1) or midbrain-hindbrain boundary. Orthodenticle homeobox 2 (*Otx2*) and gastrulation brain homeobox 2 (*Gbx2*) are among the earliest genes expressed in the neuroectoderm, dividing it into anterior and posterior domains with a border that marks the isthmus. *Otx2* is required for the development of the forebrain and midbrain, and *Gbx2* for the anterior hindbrain (Millet et al., 1999). The isthmus, at the junction of *Otx* and *Gbx* expressing areas, is a multi-signaling center regulating genes essential for the early development of both the mesencephalon and cerebellar primordium (Joyner et al., 2000, Wurst and Bally-Cuif, 2001).

The cerebellar primordium contains two distinct germinal zones, which are responsible for cerebellar neurogenesis and gliogenesis; the ventrally-located ventricular zone (VZ) and dorsally-located rhombic lip (Fink et al., 2006). Early studies on the development of CN indicated that both glutamatergic and GABAergic CN neurons originate from the cerebellar VZ (Voogd and Glickstein, 1998). Further studies highlighted the involvement of the rhombic lip as an origin for glutamatergic CN neurons (between E9-E12) (Fink et al., 2006, Wang and Zoghbi, 2001a, Green and Wingate, 2014, Machold and Fishell, 2005, Kebschull et al., 2023). LIM homeobox transcription factor 1 alpha (LMX1A) regulates the development of glutamatergic CN neurons originating from the rhombic lip. It is also expressed in the nuclear transitory zone (NTZ) and is considered to be a marker for the majority of rhombic lip-derived CN neurons in addition to a subset of LMX1A positive cells that do not originate from the rhombic lip migratory stream (Chizhikov et al., 2006, Chizhikov et al., 2010).

In this report, we provide evidence that a subset of CN neurons expressing OTX2, SNCA, MEIS2, and p75 Neurotrophin Receptor (p75NTR)/Nerve Growth Factor Receptor (NGFR) originate from the rostral end of the cerebellar primordium and are positioned in the rostroventral region of the NTZ during early cerebellar development. Our data suggest that the mesencephalon could represent a third germinal zone and, as such, the origin of previously unrecognized neurons that contribute to CN formation and development.

RESULTS

In mouse embryos, the earliest neuronal populations, which are located at the rostral end of the cerebellar primordium, are immunopositive for neurofilament-associated antigens (NAA) 3A10, a marker typically expressed in neuronal somata and axons (Marzban et al., 2008, Marzban et al., 2019) (Fig. 1). To further explore these cells in the rostral end of the cerebellar primordium, we used an antibody to detect SNCA, which is expressed in CN neurons during embryogenesis (Zhong et al., 2010). In sagittal sections of the E9 cerebellar primordium, we identified SNCA$^+$ neurons at the rostral end of the NTZ (Fig. 1E-F and Fig. Suppl. 4). To determine the location of the SNCA$^+$ cells and compare it to that of the rhombic lip-derived LMX1A$^+$ CN neurons (E10-12) in the NTZ, double immunofluorescence labeling of SNCA and LMX1A was performed on sagittal sections of E12 cerebellar primordium (Fig. 2 A-D, medial section and Fig. E-H, lateral section). This shows that an LMX1A$^+$ population of CN neurons, originating from the rhombic lip, either flanks SNCA$^+$ neurons in the medial section (Fig. 2A-D) or is located dorsally in the lateral section (Fig. 2E-H) in the NTZ. To further explore the characteristics of SNCA$^+$ cells, double immunofluorescence labeling with OTX2 and SNCA was performed during early cerebellar development. OTX2 is highly expressed in the mesencephalon and its caudal limit coincides with the boundary of the rhombencephalon (i.e., the isthmus) (Kurokawa et al., 2004). Interestingly, results from double immunofluorescence experiments in sagittal sections of E12 cerebella showed that OTX2 was highly

expressed in the mesencephalon (Fig. 3A, B), and was co-expressed with $SNCA^+$ cells in the rostral region of the cerebellar primordium (Fig. 3 A-E). Next, we used quantitative flow cytometry analysis to determine whether $OTX2^+$ cells co-express SNCA and/or LMX1A (Fig. 3F, G). An increase in the number of OTX2 and SNCA positive cells was observed at E14 in comparison to E12 (*p<0.05). The majority of neural cells were not $SNCA^+/LMX1A^+$, consistent with our IHC findings, or $SNCA^+/OTX2^+$, with the exception of a few cells that did show co-labeling. Of note, more $SNCA^+/OTX2^+$ than $SNCA^+/LMX1A^+$ cells were detected at E12 compared to E14.

IHC performed on sagittal sections of E12 to E15 cerebella showed that $OTX2^+$ cells are present at the rostral end of the cerebellar primordium (Fig. 4 A-F). To evaluate the number of $OTX2^+$ cells in the developing rostral cerebellum, the total number of $OTX2^+$ cells in the cerebellar primordium sections were counted from E12 to E15 (Fig. 4G). A comparison between these embryonic stages indicated a slight increase in the number of OTX2+ cells between E12 and E15. Significant differences were observed between E12 and E14 (**p<0.01), E12 and E15 (***p<0.001), as well as E13 and E15 (#p<0.05).

To confirm the presence of $OTX2^+$ cells in the rostral end of the cerebellar primordium, we used *Otx2*-GFP transgenic mice and performed double immunofluorescence labeling with OTX2 and GFP on E13 sagittal sections (Fig. 5). Results showed that an extension of OTX2-GFP positive cells, highly prevalent in the mesencephalon, crossed the isthmus and terminated in the rostral end of the cerebellar primordium in the NTZ (Fig. 5B, C, and D). To further validate our observations, we employed RNAscope fluorescence *in situ* hybridization (FISH) at E12 to detect the presence of *Otx2* mRNA in the cerebellar primordium (Fig. 5 E-J). *Otx2* mRNA was highly expressed in the mesencephalon and caudally extended to the rostral cerebellar primordium in the NTZ (Fig. 5 E-J and Suppl. Fig. 4).

To evaluate whether $OTX2^+$ cells are present in the absence of *Snca* gene expression, we used $Pap^{-/-}$; $Snca^{-/-}$ mice. OTX2 immunoperoxidase staining showed that even in the absence of *Snca* expression, $OTX2^+$ cells still terminated in the rostral cerebellar primordium (Suppl. Fig. 1). Nerve growth factor

receptor (p75NTR; Ngfr), which regulates neuronal proliferation and differentiation (Jiang et al., 2008, Bernabeu and Longo, 2010, Dechant and Barde, 2002), has also been shown to be expressed in the rostral end of the cerebellar primordium in Pap$^{-/-}$; Snca$^{-/-}$ mice (Rahimi-Balaei et al., 2019b). To determine whether SNCA^{+} neurons are p75NTR immunopositive, double immunolabeling with SNCA and p75NTR was performed. Section IHC revealed that SNCA^{+} cells in the NTZ exhibited cell membrane expression of p75NTR (Fig. 6A–D). This data was further confirmed by Western blot analysis of SNCA and p75NTR protein expression in embryonic cerebellar lysates (E11, 13 and 15; Fig. 6d). In addition, to conclusively determine that p75NTR is expressed in the membranes of SNCA^{+} cells, we utilized primary dissociated cultures of cerebellum at E10, DIV 4 (Fig. 6E-H). IHC demonstrated that p75NTR was indeed expressed in the membranes of SNCA^{+} cells (with punctate appearance, Fig. 6E–H (Dechant and Barde, 2002)).

To determine whether OTX2 and SNCA immunopositive cells exist in the absence of rhombic lip-derived CN neurons, we used Atoh1$^{-/-}$ mice (Fig. 7 A-C). Immunostaining revealed the presence of SNCA^{+} and OTX2^{+} cells at the rostral end of the cerebellar primordium in these animals. To validate our findings, we evaluated MEIS2, a transcription factor typically expressed in the NTZ, in Atoh1$^{+/+}$ and Atoh1$^{-/-}$ sagittal sections of the cerebellar primordium at E12. Notably, our results show the presence of two distinct sets of MEIS2^{+} cells in the NTZ of Atoh1$^{+/+}$ embryos: rhombic lip-derived CN neurons located in the caudodorsal region, which do not express SNCA (MEIS2^{+}/SNCA^{-}), and a subset of MEIS2^{+}/SNCA^{+} CN neurons situated in the rostroventral region of the NTZ (Fig. 7D-I). In Atoh1$^{-/-}$ sections, MEIS2^{+}/SNCA^{+} cells were still present in the rostroventral region of the NTZ, whereas the subpopulation of MEIS2^{+}/SNCA^{-} rhombic lip-derived CN neurons was absent in the caudodorsal region of the NTZ (Fig. 7 J-O).

To explore if the rostroventral subset of CN neurons derived from an external cerebellar germinal zone, possibly the mesencephalon, we utilized FAST DiI as a neuronal tracer to mark cells within a potential source region. FAST DiI was applied to the dorsum of the caudal mesencephalon at E9, where

it was maintained for 4 days (Fig. 8 A, a). At DIV 4, cells stained with DiI in the dorsum of the mesencephalon were present in both rostral (Fig. 8B) and caudal (Fig. 8C) directions. Sections from the cerebellar primordium revealed the presence of DiI-labeled cells within the cultured embryo (Fig. Suppl. 2). To investigate the earliest DiI-positive cell population in the mesencephalon and avoid unwanted cell staining due to long DiI exposure, we focused on early cerebellar development at E9; it has been reported that one of the premier neuronal populations in the CNS is present at this time in the mesencephalon and projects caudally (Stainier and Gilbert, 1990, Easter et al., 1993). To determine if an early generation of mesencephalic DiI-labeled cells is present within the cerebellar primordium, we limited cellular DiI exposure to only 24 hours (Fig. 8 D, d), after which it was removed (Fig. Suppl. 3). Intriguingly, almost all DiI^{+} cells migrated caudally and presented in the cerebellar primordium (Fig. 8E, e and Fig. Suppl. 3). DiI staining was clear and strong in cells as shown in Fig. 8 E, e and Fig. Suppl. 3 (arrowhead); it should be noted, however, that some DiI staining was evident in other cells in the rostral end of the cerebellar primordium, although the signal appeared relatively weak (Suppl. Fig. 3).

DISCUSSION

Previously, it was commonly held that all CN neurons had a singular origin in the ventricular zone (Pierce, 1975, Miale and Sidman, 1961). However, recent discoveries have challenged this notion, revealing a dual origin for CN neurons. Some originate from the ventricular zone, while others arise from the rhombic lip (Wang and Zoghbi, 2001b, Wang et al., 2005, Ben-Arie et al., 1997). Genetic fate mapping further suggested that most glutamatergic CN projection neurons may arise from the rhombic lip (Ben-Arie et al., 1997, Machold and Fishell, 2005, Fink et al., 2006). Transcription factor expression patterns indicate that CN neurons migrate from the rhombic lip to the NTZ through a subpial stream pathway, while sequentially expressing the genes *Lmx1a*, *Pax6*, *Tbr2*, and *Tbr1* (Fink et al., 2006).

In this study, we characterized a subset of CN neurons that do not originate from the cerebellar primordium germinal zones during early cerebellar development. We demonstrated a newly identified subset of CN neurons, which are SNCA^{+}/ OTX2^{+}/ MEIS2^{+}/ p75NTR^{+}/ LMX1A^{-}, in the rostroventral region of the NTZ in the rostral end of the cerebellar primordium. This suggests the existence of a new germinal zone during cerebellar neurogenesis.

The exact origin of the SNCA^{+}/ OTX2^{+}/ MEIS2^{+}/ p75NTR^{+}/ LMX1A^{-} CN neurons is currently unclear; however, they do not originate from the rhombic lip or ventricular zones. Rhombic lip-derived *Tbr1*$^{+}$/*Lmx1a*$^{+}$ CN neurons are born at E9, but do not reach the NTZ until ~E11 (Kebschull et al., 2023, Machold and Fishell, 2005, Wang et al., 2005, Manto et al., 2012, Fink et al., 2006, Rahimi-Balaei et al., 2018). Our results revealed that SNCA^{+} cells are a group of differentiating neurons (NAA 3A10^{+}) present in the NTZ at E9, before the arrival of any neurons that originate from the rhombic lip. The majority of SNCA^{+} CN neurons are not LMX1A^{+}; however, a small proportion of cells seems to exhibit co-expression. This suggests that in the early stages of CN neurogenesis, the pattern of protein expression in SNCA^{+} neurons may be changing, possibly with respective down- and upregulation of *Snca* and *Lmx1a*$^{+}$. Conversely, this may not occur at all, and ‘co-labeling’ could have been observed due to overlapping cells. A similar display of SNCA expression has recently been demonstrated in oligodendrocyte development and maturation (Djelloul et al., 2015). Our findings indicated that CN neuron somata are highly positive for SNCA until E14, after which SNCA expression is refined to PCs at P0 (Zhong et al., 2010) and axonal projections, indicating that SNCA^{+} cells at the rostral end of the cerebellar primordium are associated with CN establishment in the NTZ. Our results from studies using Pap$^{-/-}$; *Snca*$^{-/-}$ mice showed that lack of SNCA during cerebellar development did not affect the rostroventral subset of CN neurons (Rahimi-Balaei et al., 2019a), which still expressed OTX2 and terminated in the rostral cerebellar primordium. In adult mice, postnatal expression of SNCA has been reported in medial CN neurons (Fujita et al., 2020).

Furthermore, our observations reveal the expression of MEIS2 in the NTZ (Fig. 7 and (Morales and Hatten, 2006)), along with several other NTZ markers such as POU3F1, BRN2, IRX3, and MEIS1 as documented in (Kebschull et al., 2023, Wu et al., 2022), c-Ret and Tlx3 (Fig. Suppl. 4), indicating the existence of discrete subpopulations of precursors within the CN. MEIS2 (homeobox transcription regulator) is expressed in the mesencephalic alar plate of both mice (Cecconi et al., 1997) and chicks (Agoston and Schulte, 2009, Bobak et al., 2009). MEIS2 plays a crucial role in the development of cranial nerves and craniofacial structures (Machon et al., 2015). It has been suggested that mesencephalon development is regulated by Meis2 cross-talk with Otx2 (Agoston and Schulte, 2009). Notably, the expression of MEIS2 in CN neurons is remarkably distinct, allowing for a clear demarcation of the caudodorsal ($SNCA^-/MEIS2^+$) and rostroventral ($SNCA^+/MEIS2^+$) regions of the NTZ, whether originating from the rhombic lip or not (Fig. 7D-I). CN neurons derived from the rhombic lip require ATOH1 expression, as they are absent in an Atoh1-null mutant (Wang et al., 2005, Machold and Fishell, 2005, Zordan et al., 2008, Florio et al., 2012, Ben-Arie et al., 1997). In the Atoh1-null cerebellar primordium, the caudodorsal ($SNCA^-/MEIS2^+$) subset of CN is absent in the NTZ, while the rostroventral ($SNCA^+/MEIS2^+$) population is still present, indicating that the $Meis2^+$ rostroventral subset of the CN in the NTZ develops independently from Atoh1.

What are the potential origins of $SNCA^+$/ $OTX2^+$/ $MEIS2^+$/ $p75NTR^+$/ $LMX1A^-$ cells in the NTZ during the early stages of cerebellar development? Our study suggests that the origin of these cells may be guided by a continuous flow of rostroventral cells toward the rostral end (mesencephalon), and caudodorsal cells toward the caudal end (rhombic lip) of the cerebellar primordium. It is well established that *Otx2* is required for the development of the fore- and midbrain, while *Gbx2* is necessary for anterior hindbrain development (Simeone et al., 1992, Alvarado-Mallart, 2005, Li and Joyner, 2001, Joyner et al., 2000). The expression of OTX2 in the rostral and GBX2 in the caudal neural tube, is considered limited to the mesencephalon/metencephalon boundary (isthmus) (Alvarado-Mallart, 2005). However, a study by

Martinez *et al.* on chick/quail chimeras determined that the rostral portion of the cerebellar primordium is located more rostrally in the so-called 'mesencephalic' alar plate (Martinez and Alvarado-Mallart, 1989). Recently, *Isl1* positive cells in the anterior cerebellum were shown to exhibit residual OTX2 protein activity (Wizeman et al., 2019). Several other studies have shown that rostral cerebellar development is associated with factors expressed in the caudal mesencephalon, such as engrailed family En1 and -2 (Joyner et al., 1991, Hanks et al., 1995, Millen et al., 1995), and Acp2 (Bailey et al., 2013, Bailey et al., 2014), which are regulated by the multi-signaling center known as the isthmic organizer (Martinez et al., 2013). Furthermore, by employing embryonic cultures in conjunction with DiI labeling, we determined that the source of the rostroventral subset of CN neurons appears to be an external cerebellar germinal zone, possibly originating from the mesencephalon, which is in line with other studies (Nichols and Bruce, 2006, Wizeman et al., 2019). While our current study hints at the possibility of the caudal mesencephalon serving as a novel extrinsic germinal zone for the cerebellar primordium, further investigation is required. Genetic inducible fate mapping and long-term follow-up studies are essential to gain a comprehensive understanding of the origin, fate, and connectivity of, as well as the role played by the $SNCA^+$/ $OTX2^+$/ $MEIS2^+$/ $p75NTR^+$/ $LMX1A^-$ rostroventral subset of CN neurons in the development of the cerebellum.

In conclusion, our study indicates that the $SNCA^+$/ $OTX2^+$/ $MEIS2^+$/ $p75NTR^+$/ $LMX1A^-$ rostroventral subset of CN neurons do not originate from the well-known distinct germinative zones of the cerebellar primordium. Instead, our findings suggest the existence of a previously unidentified extrinsic germinal zone, potentially the mesencephalon.

MATERIAL AND METHODS

Animal maintenance

All animal procedures were performed in accordance with institutional regulations and the *Guide to the Care and Use of Experimental Animals* from the Canadian Council for Animal Care. For this study,

we used embryos from 47 CD1 timed-pregnant mice at embryonic day (E) 9 to E18 (total number of embryos was 409). Our approach to sample size was to include enough samples to reach a sufficient level, which was determined empirically (in most of the experiments, n was equal to 9).Timed-pregnant, prostatic acid phosphatase (PAP) mutant (*Pap*$^{-/-}$) (Zylka et al., 2008, Hokin and Hokin, 1959) mice were used at E12, because they do not express *Snca* (*Pap*$^{-/-}$ *;Snca*$^{-/-}$) and are a valuable experimental tool to assess whether SNCA is required in the development of the CN neurons (Rahimi-Balaei et al., 2019b). In addition, we studied GFP-tagged Otx2 mouse embryos (from Thomas Lamonerie lab at Université Côte d'Azur), a reporter mouse line in which the Otx2 protein is fused to the fluorescence protein GFP (Otx2$^{\text{Otx2-GFP/+}}$; (Fossat et al., 2007)). The animal procedures related to GFP-tagged Otx2 mouse embryos were in accordance with Université Côte d'Azur Institutional Animal Care and Use Committee guidelines. *Atoh1* knockout embryos were provided by Dr. Huda Zoghbi at the Baylor College of Medicine. The mice were bred, phenotyped, and genotyped (by the Zoghbi lab) according to the previously described protocol (Wang et al., 2005). Animal procedures involving Atoh1 knockout mice were in accordance with The Baylor college of Medicine Institutional Animal Care and Use Committee guidelines.

All timed-pregnant CD1 mice were obtained from the Central Animal Care Service, University of Manitoba. Animals were housed at room temperature and relative humidity (18–20°C, 50–60%) on a light:dark cycle (12:12 h) with free access to food and water. The embryonic age was determined by referencing the morning after the detection of a vaginal plug following overnight mating, considered to be E 0.5. CD1 timed-pregnant mice were anesthetized at E9, 10, 11, 12, 13, 14, 15, or 18 (+ 0.5) (n=47) using 40% isoflurane (USP, Baxter Co. Mississauga, Ontario, Canada), after which embryos were removed and prepared for Western blotting, embryonic culture, or flow cytometry analysis (FCM) or fixed in 4% paraformaldehyde (PFA) for immunohistochemistry (IHC) or neutral buffered formalin for *in situ* hybridization (ISH).

Section immunohistochemistry

Cryostat sections (20 μm) of 4% PFA fixed samples were utilized for IHC as described in our previous studies (Bailey et al., 2014, Bailey et al., 2013). Antibody dilutions were used as follows: α-synuclein 1:500 (sc-69977, Santa Cruz), p75NTR 1:1000 (8238, Cell Signaling), LMX1A 1:500 (AB10533, EMD Millipore Corporation), OTX2 1:1000 (ab114138, Abcam), NAA 1:500 (3A10, Developmental Studies Hybridoma Bank), Meis2 1:500 (ab244267, Abcam), and GFP 1:1000 (1020, Aves Labs). Fluorescent detection was performed using antibodies as follows: Streptavidin Alexa Fluor® 488 conjugate, Alexa Fluor® 568 Goat Anti-Rabbit IgG (H+L), Alexa Fluor® 488 Chicken Anti-Mouse IgG (H+L), Alexa Fluor® 488 Chicken Anti-Rabbit IgG (H + L), and Alexa Fluor® 568 Goat Anti-Mouse IgG (H+L) (S-11223, A-11036, A21200, A21441, A11004, respectively, from Life Technologies), AlexaFluro® 568 Donkey anti-goat (A-11057, invitrogen), and AlexaFluro® 647 Donkey anti-mouse (A-31571, Invitrogen), all at 1:1000. Detection of peroxidase IHC was performed as described previously (Rahimi Balaei et al., 2016, Bailey et al., 2014, Bailey et al., 2013) using HRP conjugated goat anti-rabbit IgG and goat anti-mouse IgG (H+L) antibodies (EMD Millipore Corporation, 12-348 and AP308P, respectively), both at 1:500, and developed with 3,3'-diaminobenzidine solution (DAB, Sigma, St. Louis MO, USA).

Primary dissociated cerebellum cell cultures

Primary cerebellar cultures were prepared from E10 CD1 mice, and maintained for varying 'days *in vitro'* (DIV; 1, 2, 3, 5, and 8), according to published methods (Shabanipour et al., 2019). Briefly, the entire cerebellum was removed from each embryo and immediately placed into ice cold Ca^{2+}/Mg^{2+}-free Hank's balanced salt solution (HBSS) containing gentamicin (10 μg/ml) and glucose (6 mM). Next, cerebella were incubated at 34°C for 12 min in HBSS containing 0.1% trypsin. After washing, the cerebella were gently triturated with a Pasteur transfer pipette in HBSS containing DNase I (5 U/ml) and

12 mM $MgSO_4$ until the cell mass was no longer visible. Cells were collected by centrifugation (1,200 rpm, 4°C for 5 min) and re-suspended in seeding medium (Dulbecco's modified Eagle's medium and F12, 1:1) supplemented with putrescine (100 μM), sodium selenite (30 nM), L-glutamine (1.4 mM), gentamicin (5 μg/ml), and 10% heat-inactivated fetal bovine serum. Cells were seeded on poly-L-ornithine coated glass coverslips (12 mm) at a density of 5×10^6 cells/ml, and each coverslip was placed into an individual well of a 24-well plate. After 6–8 h incubation in a CO_2 incubator (95% humidity, 37°C, 5% CO_2) to accomplish cell adherence, 500 μl of culture medium supplemented with transferrin (200 μg/ml), insulin (20 μg/ml), progesterone (40 nM), and triiodothyronine (0.5 ng/ml) was added to each culture well. After 7 days, half of the medium in each dish was replaced with fresh medium that was additionally supplemented with cytosine arabinoside (4 μM) and bovine serum albumin (100 μg/ml) (Bailey et al., 2013, Marzban and Hawkes, 2007, Marzban et al., 2003).

Embryonic cultures and DiI labeling of cells within the mesencephalon

Embryonic cultures were prepared from E9 and E10 CD1 timed-pregnant mice, and maintained for various DIV (4 and 6). Each embryo was removed from the amniotic sac and immediately placed into ice cold Ca^{2+}/Mg^{2+}-free HBSS containing gentamicin (10 μg/ml) and glucose (6 mM). Embryos were placed into 24-well plates in culture medium plus 10% fetal bovine serum and incubated in a CO_2 incubator (95% humidity, 37°C, 5% CO_2) (Marzban and Hawkes, 2007). During incubation, embryos were monitored every 6 h to evaluate the heartbeat (as an indicator of survival). On DIV 4 or 6, each well was fixed with 4% PFA and prepared for whole mount IHC.

For neuronal tracing and labeling, we used FAST DiI crystal (FAST DiI™ solid; DiIΔ9,12-C18(3), CBS (1,1'-Dilinoleyl-3,3,3',3'-Tetramethylindocarbocyanine, 4-Chlorobenzenesulfonate, D7756, Fisher Scientific). Briefly, FAST DiI was inserted into the mesencephalon at E9 using a sharp-ended needle (30g). After insertion of FAST DiI, images were captured by a stereomicroscope to assess the location of

DiI at DIV 0. After placing the embryos into 24-well plates in culture medium, they were monitored every 6 hours and fixed with 4% PFA on the desired day. Next, whole mount IHC with neurofilament-associated antigen (NAA 3A10) was performed to visualize neural fiber growth, followed by sectioning and imaging of the DiI positive cells in the mesencephalon and cerebellar primordium.

Fluorescent in situ hybridization (FISH)-RNAscope

All of the ISH experiments were carried out using E12 CD1 mice, in which the cerebellar primordium is well established, using RNAscope ACD HybEZ™ II Hybridization System and RNAscope® Multiplex Fluorescent Reagent Kit v2 (Advanced Cell Diagnostics, Hayward, CA, USA). Briefly, embryos were fixed in 10% (vol/vol) neutral buffered formalin at room temperature for 24 h, dehydrated, and embedded in paraffin. Tissue sections cut at 10 μm thickness were processed for RNA *in situ* detection according to the manufacturer's user manual. The sequence of the probe used in this study was Mm-*Otx2*-C3 (444381, ACD); cyanine 3 (NEL744E001KT; TSA® Plus, Perkin Elmers, Waltham, MA, USA) was used as the fluorophore.

Western blot analyses

Equal amounts of total protein were separated by SDS/PAGE in 10–15% precast gels (Bio-Rad, Hercules, CA, USA) and transferred onto PVDF-membranes. For Western blot analysis, membranes were blocked in 5% nonfat dry milk (NFDM) in TBS containing 0.02% Tween 20 (TBST) for 1hour at RT and subsequently incubated overnight at 4°C with primary antibodies [α-synuclein (sc-69977, Santa Cruz, 1:2000) or p75NTR (8238, Cell Signaling, 1:1000), all dilutions in blocking buffer]. After washing with TBST, membranes were exposed to secondary antibodies [HRP conjugated goat anti-mouse IgG (AP308P, Millipore, 1:6000) or HRP conjugated goat anti-rabbit IgG (12-348, Millipore, 1:6000)]. Bands

were visualized using the enhanced chemiluminescence (ECL) protocol on scientific imaging film. All bands were normalized to β-actin expression.

Counting of OTX2 positive cells

To assess the number of OTX2-positive cells, we conducted immunohistochemistry (IHC) labeling on slides containing serial sections from embryonic days 12, 13, 14, and 15 (n=3 at each timepoint). Under the microscope, we systematically counted OTX2-positive cells within the cerebellar primordium. This analysis encompassed a minimum of 10 sections, spread across at least 3 slides, ensuring comprehensive coverage of OTX2 expression along the mediolateral axis of the cerebellar primordium. For each slide, the counts of OTX2-positive cells from all sections were cumulatively calculated to determine the total number of positive cells per slide. Subsequently, statistical analysis was employed to compare the results obtained at different developmental time points.

Flow cytometry analysis

After dissociation (see primary dissociated cerebellar cell culture section), cells were fixed in 4% PFA. Each group consisted of 350,000 cells and all procedures before sorting were performed at room temperature. Primary antibodies used: α-synuclein 1:500 (sc-69977, Santa Cruz), LMX1A 1:1000 (AB10533, EMD Millipore Corporation), and OTX2 1:500 (ab114138, Abcam). Fluorescent detection was performed using antibodies as follows: Alexa Fluor 488 Chicken Anti-Rabbit IgG (H / L) and Alexa Fluor 568 Goat Anti-Mouse IgG (H+L) (A21441 and A11004, respectively, from Life Technologies), both at 1:750. Cells were pelleted by centrifugation, washed, and resuspended in 200 µL staining buffer (1X PBS contains 1% FBS and 1mM EDTA). Data were acquired on a CytoFlex-LX flow cytometer (Beckman Coulter) equipped with 355, 375, 405, 488, 561, 638 and 808 Laser lines using CytExpert

software, and analyzed with Flow Jo (version 10, Treestar, San Carlos, CA) at the University of Manitoba flow cytometry core facility. Cellular debris was excluded using forward light scatter/side scatter plot.

Imaging and figure preparation

For bright field microscopy, images were captured using a Zeiss Axio Imager M2 microscope and subsequently analyzed with Zeiss Microscope Software (Zen Image Analyses software; Zeiss, Toronto, ON, Canada). For fluorescence microscopy of entire cerebellar sections, a Zeiss Lumar V12 Fluorescence stereomicroscope (Zeiss, Toronto, ON, Canada) equipped with a camera was used; captured images were analyzed using Zen software. For high magnification fluorescence microscopy, a Zeiss Z1 and Z2 Imager and a Zeiss LSM 700 confocal microscope (Zeiss, Toronto, ON, Canada) equipped with camera and Zen software were used to capture and analyze images. Images were cropped, corrected for brightness and contrast, and assembled into montages using Adobe Photoshop CS5 Version 12.

Statistical analysis

Data on OTX2 positive cell counts are presented as the mean ± standard error of mean (SEM) from n separate experiments. Statistical significance of differences was evaluated by One-Way ANOVA followed by a Tukey`s multiple comparison test. Differences were considered statistically significant when $P<0.05$. All statistical analyses were performed using GraphPad Prism 6 software for Windows.

ACKNOWLEDGEMENTS:

The authors would like to acknowledge Dr. Christine Zhang and Mr. Gerald Stelmack for their technical assistance, and Science Impact (Winnipeg, Canada) for (post-)editing the manuscript.

COMPETING INTEREST:

The authors have no conflicts of interest.

FUNDING:

This study was supported by grants from the Natural Sciences and Engineering Research Council (HM: NSERC Discovery Grant # RGPIN-2018-06040), The Children's Hospital Research Institute of Manitoba (HM: CHRIM Grant # 320035), Research Manitoba Tri-Council Bridge Funding Program (HM: Grant # 47955), and University Collaborative Research Program (UCRP).

REFERENCES

AGOSTON, Z. & SCHULTE, D. 2009. Meis2 competes with the Groucho co-repressor Tle4 for binding to Otx2 and specifies tectal fate without induction of a secondary midbrain-hindbrain boundary organizer. *Development,* 136**,** 3311-22.

ALVARADO-MALLART, R. M. 2005. The chick/quail transplantation model: discovery of the isthmic organizer center. *Brain Res Brain Res Rev,* 49**,** 109-13.

BAILEY, K., RAHIMI BALAEI, M., MANNAN, A., DEL BIGIO, M. R. & MARZBAN, H. 2014. Purkinje cell compartmentation in the cerebellum of the lysosomal Acid phosphatase 2 mutant mouse (nax - naked-ataxia mutant mouse). *PLoS One,* 9**,** e94327.

BAILEY, K., RAHIMI BALAEI, M., MEHDIZADEH, M. & MARZBAN, H. 2013. Spatial and temporal expression of lysosomal acid phosphatase 2 (ACP2) reveals dynamic patterning of the mouse cerebellar cortex. *Cerebellum,* 12**,** 870-81.

BEN-ARIE, N., BELLEN, H. J., ARMSTRONG, D. L., MCCALL, A. E., GORDADZE, P. R., GUO, Q., MATZUK, M. M. & ZOGHBI, H. Y. 1997. Math1 is essential for genesis of cerebellar granule neurons. *Nature,* 390**,** 169-72.

BERNABEU, R. O. & LONGO, F. M. 2010. The p75 neurotrophin receptor is expressed by adult mouse dentate progenitor cells and regulates neuronal and non-neuronal cell genesis. *BMC neuroscience,* 11**,** 1.

BOBAK, N., AGOSTON, Z. & SCHULTE, D. 2009. Evidence against involvement of Bmp receptor 1b signaling in fate specification of the chick mesencephalic alar plate at HH16. *Neurosci Lett,* 461**,** 223-8.

CECCONI, F., PROETZEL, G., ALVAREZ-BOLADO, G., JAY, D. & GRUSS, P. 1997. Expression of Meis2, a Knotted-related murine homeobox gene, indicates a role in the differentiation of the forebrain and the somitic mesoderm. *Dev Dyn,* 210**,** 184-90.

CHIZHIKOV, V., STESHINA, E., ROBERTS, R., ILKIN, Y., WASHBURN, L. & MILLEN, K. J. 2006. Molecular definition of an allelic series of mutations disrupting the mouse Lmx1a (dreher) gene. *Mammalian genome,* 17**,** 1025-1032.

CHIZHIKOV, V. V., LINDGREN, A. G., MISHIMA, Y., ROBERTS, R. W., ALDINGER, K. A., MIESEGAES, G. R., CURRLE, D. S., MONUKI, E. S. & MILLEN, K. J. 2010. Lmx1a regulates fates and location of cells originating from the cerebellar rhombic lip and telencephalic cortical hem. *Proceedings of the National Academy of Sciences,* 107**,** 10725-10730.

DECHANT, G. & BARDE, Y.-A. 2002. The neurotrophin receptor p75NTR: novel functions and implications for diseases of the nervous system. *Nature neuroscience,* 5**,** 1131-1136.

DJELLOUL, M., HOLMQVIST, S., BOZA-SERRANO, A., AZEVEDO, C., YEUNG, M. S., GOLDWURM, S., FRISÉN, J., DEIERBORG, T. & ROYBON, L. 2015. Alpha-synuclein expression in the oligodendrocyte lineage: an in vitro and in vivo study using rodent and human models. *Stem cell reports,* 5**,** 174-184.

EASTER, S. S., JR., ROSS, L. S. & FRANKFURTER, A. 1993. Initial tract formation in the mouse brain. *J Neurosci,* 13**,** 285-99.

FINK, A. J., ENGLUND, C., DAZA, R. A., PHAM, D., LAU, C., NIVISON, M., KOWALCZYK, T. & HEVNER, R. F. 2006. Development of the deep cerebellar nuclei: transcription factors and cell migration from the rhombic lip. *The Journal of neuroscience,* 26**,** 3066-3076.

FLORIO, M., LETO, K., MUZIO, L., TINTERRI, A., BADALONI, A., CROCI, L., ZORDAN, P., BARILI, V., ALBIERI, I., GUILLEMOT, F., ROSSI, F. & CONSALEZ, G. G. 2012. Neurogenin 2 regulates progenitor cell-cycle progression and Purkinje cell dendritogenesis in cerebellar development. *Development,* 139**,** 2308-20.

FOSSAT, N., LE GRENEUR, C., BEBY, F., VINCENT, S., GODEMENT, P., CHATELAIN, G. & LAMONERIE, T. 2007. A new GFP-tagged line reveals unexpected Otx2 protein localization in retinal photoreceptors. *BMC Dev Biol,* 7**,** 122.

FUJITA, H., KODAMA, T. & DU LAC, S. 2020. Modular output circuits of the fastigial nucleus for diverse motor and nonmotor functions of the cerebellar vermis. *Elife,* 9.

GOLDOWITZ, D. & HAMRE, K. 1998. The cells and molecules that make a cerebellum. *Trends in neurosciences,* 21**,** 375-382.

GREEN, M. J. & WINGATE, R. J. 2014. Developmental origins of diversity in cerebellar output nuclei. *Neural Dev,* 9**,** 1.

HANKS, M., WURST, W., ANSON-CARTWRIGHT, L., AUERBACH, A. B. & JOYNER, A. L. 1995. Rescue of the En-1 mutant phenotype by replacement of En-1 with En-2. *Science,* 269**,** 679-82.

HOKIN, M. R. & HOKIN, L. E. 1959. The synthesis of phosphatidic acid from diglyceride and adenosine triphosphate in extracts of brain microsomes. *Journal of Biological Chemistry,* 234**,** 1381-1386.

JIANG, X., GWYE, Y., MCKEOWN, S. J., BRONNER-FRASER, M., LUTZKO, C. & LAWLOR, E. R. 2008. Isolation and characterization of neural crest stem cells derived from in vitro–differentiated human embryonic stem cells. *Stem cells and development,* 18**,** 1059-1071.

JOYNER, A. L., HERRUP, K., AUERBACH, B. A., DAVIS, C. A. & ROSSANT, J. 1991. Subtle cerebellar phenotype in mice homozygous for a targeted deletion of the En-2 homeobox. *Science,* 251**,** 1239-43.

JOYNER, A. L., LIU, A. & MILLET, S. 2000. Otx2, Gbx2 and Fgf8 interact to position and maintain a mid–hindbrain organizer. *Current opinion in cell biology,* 12**,** 736-741.

KEBSCHULL, J. M., CASONI, F., CONSALEZ, G. G., GOLDOWITZ, D., HAWKES, R., RUIGROK, T. J. H., SCHILLING, K., WINGATE, R., WU, J., YEUNG, J. & UUSISAARI, M. Y. 2023. Cerebellum Lecture: the Cerebellar Nuclei-Core of the Cerebellum. *Cerebellum*.

KUROKAWA, D., KIYONARI, H., NAKAYAMA, R., KIMURA-YOSHIDA, C., MATSUO, I. & AIZAWA, S. 2004. Regulation of Otx2 expression and its functions in mouse forebrain and midbrain. *Development,* 131**,** 3319-3331.

LI, J. Y. & JOYNER, A. L. 2001. Otx2 and Gbx2 are required for refinement and not induction of mid-hindbrain gene expression. *Development,* 128**,** 4979-4991.

MACHOLD, R. & FISHELL, G. 2005. Math1 is expressed in temporally discrete pools of cerebellar rhombic-lip neural progenitors. *Neuron,* 48**,** 17-24.

MACHON, O., MASEK, J., MACHONOVA, O., KRAUSS, S. & KOZMIK, Z. 2015. Meis2 is essential for cranial and cardiac neural crest development. *BMC Dev Biol,* 15**,** 40.

MANTO, M., GRUOL, D. L., SCHMAHMANN, J. D., KOIBUCHI, N. & ROSSI, F. 2012. *Handbook of the cerebellum and cerebellar disorders,* New York, Springer.

MARTINEZ, S. & ALVARADO-MALLART, R. M. 1989. Rostral cerebellum originates from the caudal portion of the so-called ‘mesencephalic’vesicle: a study using chick/quail chimeras. *European Journal of Neuroscience,* 1**,** 549-560.

MARTINEZ, S., ANDREU, A., MECKLENBURG, N. & ECHEVARRIA, D. 2013. Cellular and molecular basis of cerebellar development. *Front Neuroanat,* 7**,** 18.

MARZBAN, H., DEL BIGIO, M. R., ALIZADEH, J., GHAVAMI, S., ZACHARIAH, R. M. & RASTEGAR, M. 2015. Cellular commitment in the developing cerebellum. *Frontiers in cellular neuroscience,* 8**,** 450.

MARZBAN, H. & HAWKES, R. 2007. Fibroblast growth factor promotes the development of deep cerebellar nuclear neurons in dissociated mouse cerebellar cultures. *Brain research,* 1141**,** 25-36.

MARZBAN, H., KHANZADA, U., SHABIR, S., HAWKES, R., LANGNAESE, K., SMALLA, K. H., BOCKERS, T. M., GUNDELFINGER, E. D., GORDON-WEEKS, P. R. & BEESLEY, P. W. 2003. Expression of the immunoglobulin superfamily neuroplastin adhesion molecules in adult and developing mouse cerebellum and their localisation to parasagittal stripes. *Journal of Comparative Neurology,* 462**,** 286-301.

MARZBAN, H., KIM, C.-T., DOORN, D., CHUNG, S.-H. & HAWKES, R. 2008. A novel transverse expression domain in the mouse cerebellum revealed by a neurofilament-associated antigen. *Neuroscience,* 153**,** 1190-1201.

MARZBAN, H., RAHIMI-BALAEI, M. & HAWKES, R. 2019. Early trigeminal ganglion afferents enter the cerebellum before the Purkinje cells are born and target the nuclear transitory zone. *Brain Struct Funct,* 224**,** 2421-2436.

MIALE, I. L. & SIDMAN, R. L. 1961. An autoradiographic analysis of histogenesis in the mouse cerebellum. *Exp Neurol,* 4**,** 277-96.

MILLEN, K. J., HUI, C. C. & JOYNER, A. L. 1995. A role for En-2 and other murine homologues of Drosophila segment polarity genes in regulating positional information in the developing cerebellum. *Development,* 121**,** 3935-45.

MILLET, S., CAMPBELL, K., EPSTEIN, D. J., LOSOS, K., HARRIS, E. & JOYNER, A. L. 1999. A role for Gbx2 in repression of Otx2 and positioning the mid/hindbrain organizer. *Nature,* 401**,** 161-4.

MORALES, D. & HATTEN, M. E. 2006. Molecular markers of neuronal progenitors in the embryonic cerebellar anlage. *J Neurosci,* 26**,** 12226-36.

NICHOLS, D. H. & BRUCE, L. L. 2006. Migratory routes and fates of cells transcribing the Wnt-1 gene in the murine hindbrain. *Developmental dynamics,* 235**,** 285-300.

PIERCE, E. T. 1975. Histogenesis of the deep cerebellar nuclei in the mouse: an autoradiographic study. *Brain Res,* 95**,** 503-18.

RAHIMI-BALAEI, M., BERGEN, H., KONG, J. & MARZBAN, H. 2018. Neuronal Migration During Development of the Cerebellum. *Front Cell Neurosci,* 12**,** 484.

RAHIMI-BALAEI, M., BUCHOK, M., VIHKO, P., PARKINSON, F. E. & MARZBAN, H. 2019a. Loss of prostatic acid phosphatase and alpha-synuclein cause motor circuit degeneration without altering cerebellar patterning. *PLoS One,* 14**,** e0222234.

RAHIMI-BALAEI, M., BUCHOK, M., VIHKO, P., PARKINSON, F. E. & MARZBAN, H. 2019b. Loss of prostatic acid phosphatase and α-synuclein cause motor circuit degeneration without altering cerebellar patterning. *PloS one,* 14.

RAHIMI BALAEI, M., JIAO, X., ASHTARI, N., AFSHARINEZHAD, P., GHAVAMI, S. & MARZBAN, H. 2016. Cerebellar expression of the neurotrophin receptor p75 in naked-ataxia mutant mouse. *International journal of molecular sciences,* 17**,** 115.

SHABANIPOUR, S., DALVAND, A., JIAO, X., RAHIMI BALAEI, M., CHUNG, S. H., KONG, J., DEL BIGIO, M. R. & MARZBAN, H. 2019. Primary Culture of Neurons Isolated from Embryonic Mouse Cerebellum. *J Vis Exp*.

SIMEONE, A., ACAMPORA, D., GULISANO, M., STORNAIUOLO, A. & BONCINELLI, E. 1992. Nested expression domains of four homeobox genes in developing rostral brain. *Nature,* 358**,** 687-90.

SOTELO, C. 2004. Cellular and genetic regulation of the development of the cerebellar system. *Progress in neurobiology,* 72**,** 295-339.

STAINIER, D. & GILBERT, W. 1990. Pioneer neurons in the mouse trigeminal sensory system. *Proceedings of the National Academy of Sciences,* 87**,** 923-927.

VOOGD, J. & GLICKSTEIN, M. 1998. The anatomy of the cerebellum. *Trends in cognitive sciences,* 2**,** 307-313.

WANG, V. Y., ROSE, M. F. & ZOGHBI, H. Y. 2005. Math1 expression redefines the rhombic lip derivatives and reveals novel lineages within the brainstem and cerebellum. *Neuron,* 48**,** 31-43.

WANG, V. Y. & ZOGHBI, H. Y. 2001a. Genetic regulation of cerebellar development. *Nature Reviews Neuroscience,* 2**,** 484.

WANG, V. Y. & ZOGHBI, H. Y. 2001b. Genetic regulation of cerebellar development. *Nat Rev Neurosci,* 2**,** 484-91.

WIZEMAN, J. W., GUO, Q., WILION, E. M. & LI, J. Y. 2019. Specification of diverse cell types during early neurogenesis of the mouse cerebellum. *eLife,* 8**,** e42388.

WU, J. P. H., YEUNG, J., RAHIMI-BALAEI, M., WU, S. R., ZOGHBI, H. & GOLDOWITZ, D. 2022. The Transcription Factor Pou3f1 Sheds Light on the Development and Molecular Diversity of Glutamatergic Cerebellar Nuclear Neurons in the Mouse. *Front Mol Neurosci,* 15**,** 921901.

WURST, W. & BALLY-CUIF, L. 2001. Neural plate patterning: upstream and downstream of the isthmic organizer. *Nat Rev Neurosci,* 2**,** 99-108.

ZHONG, S.-C., LUO, X., CHEN, X.-S., CAI, Q.-Y., LIU, J., CHEN, X.-H. & YAO, Z.-X. 2010. Expression and subcellular location of alpha-synuclein during mouse-embryonic development. *Cellular and molecular neurobiology,* 30**,** 469-482.

ZORDAN, P., CROCI, L., HAWKES, R. & CONSALEZ, G. G. 2008. Comparative analysis of proneural gene expression in the embryonic cerebellum. *Dev Dyn,* 237**,** 1726-35.

ZYLKA, M. J., SOWA, N. A., TAYLOR-BLAKE, B., TWOMEY, M. A., HERRALA, A., VOIKAR, V. & VIHKO, P. 2008. Prostatic acid phosphatase is an ectonucleotidase and suppresses pain by generating adenosine. *Neuron,* 60**,** 111-122.

FIGURE LEGENDS

Fig. 1. The presence of neurons in the cerebellar primordium at E9 and spatial expression of SNCA. The cerebellar primordium immunostained with NAA and SNCA, shows that a distinct subset of neurons located at the rostral end of the developing cerebellum.
A: Dorsal view of the schematic illustration of the cerebellar primordium, mesencephalon, isthmus, and 4th ventricle. The red line indicates the sagittal plane about which the sections shown in **B-D** were taken.
B-D: Sagittal section through the cerebellar primordium at early E9 immunoperoxidase-labeled with NAA 3A10 shows the presence of neurons in the cerebellar primordium that cross the isthmus (i) and continue to the mesencephalon. **C**. A higher magnification of **B. D**. Differentiated neurons at E9.5 are visible; a higher magnification is shown in the inset, **d.**
E: Sagittal section through the cerebellar primordium at late E9. Immunofluorescence labeling of SNCA shows $SNCA^+$ (green) expressing CN neurons in the mesencephalon, at the isthmus (i) and in the rostral part of the cerebellar primordium (cb). **F.** A higher magnification of **E**.
Abbreviations: 4thv, 4th ventricle; cb, cerebellum; c, caudal; d, dorsal; i, isthmus; m, mesencephalon; r, rostral; v, ventral
Scale bar = 100 µm in B; 50 µm in C and E; 20 µm in D

Fig. 2. SNCA expression relative to Lmx1a in the early developing mouse cerebellum. The sagittal section through the cerebellar primordium at E12.5 reveals double immunofluorescence labeling with SNCA and LMX1A antibodies in both medial (panels A-D) and lateral (panels E-H) sections.
A–G: SNCA (green, **A** and **E**) and LMX1A (red, **B** and **F**) immunopositive cells are located at the NTZ. $SNCA^+$ cells continue to the mesencephalon, and $LMX1A^+$ cells toward the rhombic lip. Merged images show that the $SNCA^+$ cells form a population of CN neurons distinct from the rhombic lip-derived cells ($LMX1A^+$) in the NTZ (**C** and **G**). **D** and **H** show a higher magnification of **C** and **G**, respectively.
Abbreviations: 4thV, 4th ventricle; cb, cerebellum; c, caudal; d, dorsal; i, isthmus; m, mesencephalon; rl, rhombic lip; NTZ, nuclear transitory zone; r, rostral; v, ventral.
Scale bar = 100 µm.

Fig. 3. Expression of SNCA and OTX2 in the developing cerebellar primordium. Double immunofluorescence labeling with SNCA and OTX2 antibodies in sagittal sections of the cerebellar primordium at E12.5.
A–E: Double immunolabeling of SNCA (green) and OTX2 (red) of a sagittal section of the cerebellar primordium at E12.5 **A**. High OTX2 immunoreactivity was detected in the mesencephalon. $SNCA^+$ cells in the mesencephalon accompany $OTX2^+$ cells across the isthmus (i) and in the NTZ. **B**. higher magnification of **A**. **C-E**. Immunolabeling with SNCA (green, **C**) and OTX2 (red, **D**) and merged (**E**) shows co-expression in the NTZ.
F-G: Cerebellar cells at E12 and E14 were dissociated and immunolabeled for SNCA + OTX2, SNCA + LMX1A, or each antibody individually (F). Quantitative analysis was performed by flow cytometry to

detect SNCA$^+$, OTX2$^+$, LMX1A$^+$, SNCA$^+$/ LMX1A$^+$ and SNCA$^+$/ OTX2$^+$ cells (**G**). No significant differences were observed for the number of LMX1A$^+$ cells between E12 and E14. An increase in SNCA and OTX2 positive cells was shown at E14 in comparison to E12 (*P<0.05). The number of cells positive for SNCA/LMX1A or SNCA/OTX2 was very low at E12 and E14.
Abbreviations: 4thv, 4th ventricle; cb, cerebellum; c, caudal; d, dorsal; i, isthmus; m, mesencephalon; rl, rhombic lip; NTZ, nuclear transitory zone; r, rostral; v, ventral.
Scale bar = 200 µm in A; 50 µm in B; 20 µm in C, D, and E.

Fig. 4. The spatial and temporal expression of OTX2 in the developing cerebellum of mice. Sagittal sections through the cerebellar primordia at E12, 13, 14, and 15 were analyzed for peroxidase immunoreactivity of OTX2.
A–F: Sagittal section through cerebellar primordium at E12 (**A**; higher magnification shown in **B**), E13 (**C**; higher magnification shown in **D**), E14 (**E**), and E15 (**F**). High OTX2 immunoreactivity at the mesencephalon is evident, and a few OTX2+ cells cross the isthmus and position at the rostral part of the cerebellar primordium at the NTZ. Examples of Otx2 expressing cells are indicated by arrowheads in panels B, D, E, and F. In panels E and F, the isthmus and adjacent cerebellar area are showed in the same orientation as panels A-D (I; isthmus). The orientation label (r-c and d-v; rostral caudal and dorsal ventral) in panel A applies to all panels.
G: Comparison of the number of OTX2 positive cells in the cerebellar primordium from E12 to E15. Results indicate a slight increase in the number of OTX2 positive cells over time. Significant differences were observed between E12 and E14 (**P<0.01), E12 and E15 (***P<0.001), as well as E13 and E15 (#P<0.05). Data were analyzed by One-Way ANOVA followed by a Tukey's multiple comparison test.
Abbreviations: 4thv, 4th ventricle; cb, cerebellum; c, caudal; d, dorsal; i, isthmus; m, mesencephalon; rl, rhombic lip; r, rostral; v, ventral.
Scale bar = 200 µm in A and C; 50 µm in F (applies to B, D, E, and F).

Fig. 5. Otx2 expression in developing cerebella of Otx2-GFP transgenic and control mice. Sagittal sections through the cerebellar primordium of Otx2-GFP transgenic mice at E13 are shown in panels A-D, and RNAscope fluorescence in situ hybridization (FISH) of Otx2 at E12 in wild-type mice in panels E-J.
A-D: DAPI labels the outline of the cerebellar primordium and mesencephalon (**A**, blue). GFP expression, which is enhanced by immunofluorescence labeling with anti-GFP (**B**, green), and immunofluorescence labeling for OTX2 (**C**, red), reveal co-labeled cells (**D**, merged) in the mesencephalon and NTZ at the rostral end of the cerebellar primordium. Arrows indicate the isthmus.
E-G: Merged channels of the *in situ* hybridization of *Otx2* mRNA probe counterstained with DAPI at low (**E**) and high (**F** and **G**) magnification captured by confocal microscopy.
H-J: The Otx2 mRNA signal was strong in the mesencephalon and extended as a tail through the isthmus to the rostral cerebellar primordium in the NTZ. The isthmus is indicated by arrows in (**E, F, H, I**) and a line in (**J**).
Abbreviations: cb, cerebellum; c, caudal; d, dorsal; m, mesencephalon; rl, rhombic lip; ntz, nuclear transitory zone; r, rostral; v, ventral.

Scale bar = 200 µm in D (applies to A-D); 100 µm in H (applies to E and H); 20 µm in J (applies to F - J).

Fig. 6. SNCA immunopositive cells express p75NTR (NGFR) in developing cerebellum in vivo and in vitro.
A–D: Double immunofluorescence labeling with SNCA (**A**, green) and p75NTR (**B**, red) antibodies reveals co-labeled cells (**C**, merged) in the NTZ; a higher magnification of the NTZ is shown in **D**.
d. Western blot analysis of SNCA and p75NTR expression during cerebellar development. Immunoblots of total cerebellar lysates from embryos at E11, E13 and E15 indicate an increase in expression of SNCA and p75NTR from E11 to E15. Equal protein loading was confirmed by β-actin expression.
E–H: Primary dissociated cultures of cerebellum obtained from an E10 mouse embryo (DIV 4), double immunofluorescence stained for SNCA (**E**: green) and p75NTR (**F**: red) (merged image shown in **G**). **H** is a higher magnification of **G**; punctuate cellular p75NTR immunoreactivity is marked by arrow heads.
Abbreviations: cb, cerebellum; c, caudal; d, dorsal; NTZ, nuclear transitory zone; r, rostral; v, ventral.
Scale bar = 50 µm in A–C and D–F; 20 µm in H; 10 µm in G.

Fig. 7. SNCA, OTX2, and MEIS2 expression in the developing cerebella of Atoh1 null and control mice. Sagittal sections through the cerebellar primordia of Atoh1$^{+/+}$ and Atoh1$^{-/-}$ embryos at E12.5; double immunofluorescence labeling with SNCA + OTX2 and SNCA + MEIS2 antibodies is demonstrated.
A–C: SNCA (green, **A**) and OTX2 (red, **B**) immunopositive cells are present in the mesencephalon and NTZ of Atoh1 KO mouse (merged channels, **C**).
D-F: In E12.5 Atoh1$^{+/+}$ sagittal sections, SNCA^{+} (green, **D**) cells are observed in the mesencephalon and NTZ. MEIS2^{+} (red, **E**) cells are present in the mesencephalon and NTZ in addition to another population of MEIS2^{+} cells in the dorsal region of the NTZ which extends to the rhombic lip. Merged image (**F**) confirms the presence of two distinct sets of MEIS2^{+} cells in the NTZ: rhombic lip-derived CN neurons located in the caudodorsal (cd) region, which do not express SNCA (MEIS2^{+}/SNCA^{-}), and a subset of MEIS2^{+}/SNCA^{+} CN neurons situated in the rostroventral (rv) region of the NTZ.
G-I: Higher magnification of **D-F.**
J-L: In E12.5 Atoh1$^{-/-}$ sagittal sections, the expression of SNCA (green, **J**) shows no change as compared to Atoh1$^{+/+}$, whereas Meis2 abundance (red, **K**) exhibited a different pattern. Thus, MEIS2^{+}/SNCA^{+} cells were still present in the rostroventral region of the NTZ. However, the subpopulation of MEIS2^{+}/SNCA^{-} rhombic lip-derived CN neurons were absent in the caudodorsal region of the NTZ.
M-O: Higher magnification of **J-I**.
Abbreviations: 4thV, 4th ventricle; cb, cerebellum; cd, caudodorsal; i, isthmus; m, mesencephalon; rl, rhombic lip; NTZ, nuclear transitory zone; rv, rostroventral.
Scale bar = 100 µm

Fig. 8. Labeling of mesencephalic cells during early development in mice using embryonic culture. Fast DiI was applied to an embryo at E9 and kept for 4 days (DIV 4, panels A-C) or removed after 24 hours (DIV 1, panels D-E).

A, a: Fast DiI was inserted in the mesencephalon at E9 (DIV 0), arrowhead shows insertion location of DiI crystal in the mesencephalon. The arrow indicates the isthmus. Inset "a" shows the whole embryo and indicates the site of DiI insertion.
B-C: 4 days post DiI insertion, DiI positive cells directed both rostrally to the mesencephalon (**B**) and caudally to the rostral cerebellar primordium (**C**).
D, d: Fast DiI was inserted in the mesencephalon at E9 (DIV 0) (indicated by arrowhead) and removed at DIV1, arrow shows the isthmus. Inset "d" shows the whole embryo and indicates the site of DiI insertion.
E, e: DiI positive cells present in cerebellar primordium at DIV 6 after removal of Fast DiI at DIV1.
Abbreviations: cb, cerebellum; c, caudal; d, dorsal; m, mesencephalon; r, rostral; v, ventral.
Scale bar = 500 µm in a, d; 200 µm in A, D; 100 µm in B-C, E.

Fig. 9. A schematic illustration of the developing cerebellum at ~E12, created by BioRender.com. The expression patterns of SNCA, MEIS2, and OTX2 within the cerebellar primordium indicate a subset of CN neurons with origins distinct from the rhombic lip (rl).
Abbreviations: c, caudal; d, dorsal; m, mesencephalon; ntz, nuclear transitory zone; r, rostral; rl, rhombic lip; v, ventral.

SUPPLEMENTARY FIGURES

Supplementary Figure 1. OTX2 expression persists in Snca null mice. OTX2 immunoperoxidase staining in the cerebellar primordium of $Pap^{-/-}$; $Snca^{-/-}$ mice at E12. Results show $OTX2^{+}$ cells are present in the ntz and terminate in the rostral cerebellar primordium.
Abbreviations: cb, cerebellum; I, isthmus; ntz, nuclear transitory zone
Scale bar = 50 µm

Supplementary Figure 2. Fast DiI was applied to an embryo at E9 and kept for 4 days in vitro (DIV 4), revealing labeled cells within the cerebellar primordium.
A-C: Low and high magnifications show only a few positive cells in the rostral cerebellar primordium in the NTZ at the level of the medial cerebellar section.
D-F: Low and high magnifications indicate the presence of just a few positive cells in the rostral cerebellar primordium in the NTZ at the level of the lateral cerebellar section.
Abbreviations: cb, cerebellum; c, caudal; d, dorsal; m, mesencephalon; NTZ, nuclear transitory zone; r, rostral; v, ventral.
Scale bar = 100 µm in A applies to D; 50 µm in B applies to E; 20 µm in C applies to I as well.

Supplementary Figure 3. Fast DiI was applied to the embryo at E9 and removed after 24 hours, resulting in the visualization of labeled cells within the cerebellar primordium (higher magnification in Fig. 8 E,e).
A: DiI positive cells present in cerebellar primordium at DIV 6 after removal of Fast DiI at DIV1 (indicated by arrowhead), arrow points to the isthmus.

B: A higher magnification from the caudal to mesencephalon and rostral rhombencephalon shows DiI positive cells in the cerebellar primordium, arrow points to the isthmus.
Abbreviations: cb, cerebellum; c, caudal; d, dorsal; m, mesencephalon; r, rostral; v, ventral.
Scale bar = 500 µm in B; 100 µm in C.

Supplementary Figure 4. *In situ* hybridization demonstrates expression pattern of Otx2, Snca, C-Ret, and Tlx3. These images show distribution of Otx2, Snca, C-Ret and Tlx3 in the cerebellar primordium at E11.5, E13.5 and E15.5; all markers are present in the rostroventral region of the NTZ. All images show cerebellar primordia. Image credit: Allen Institute. © 2008 Allen Institute for Brain Science. Allen Developing Mouse Brain Atlas. Available online at: https://developingmouse.brain-map.org/.

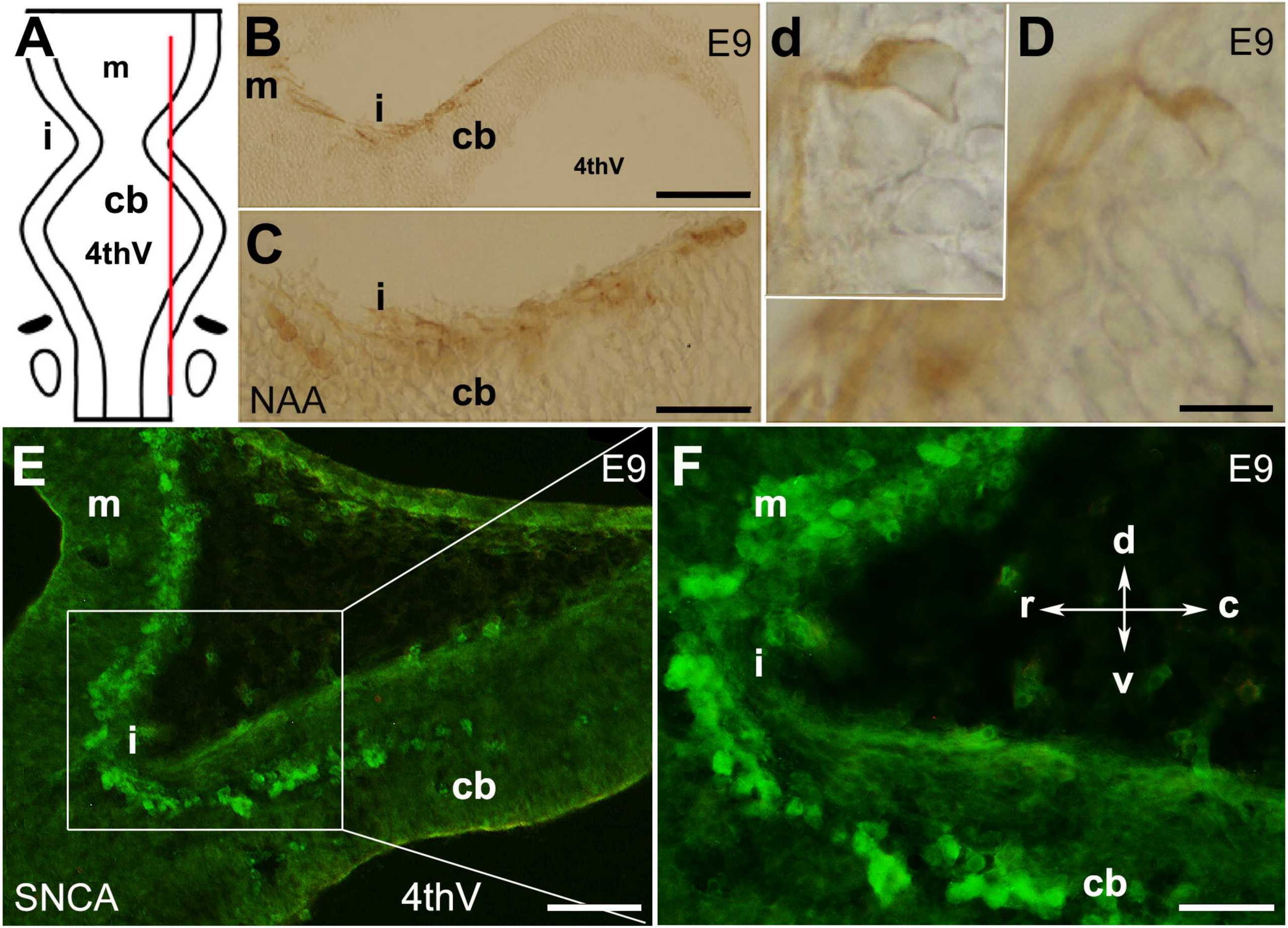
A
m
i
cb
4thV
B
E9
m
i
cb
4thV
C
i
NAA
cb
d
D
E9
E
E9
m
i
cb
SNCA
4thV
F
E9
m
d
r
c
v
i
cb

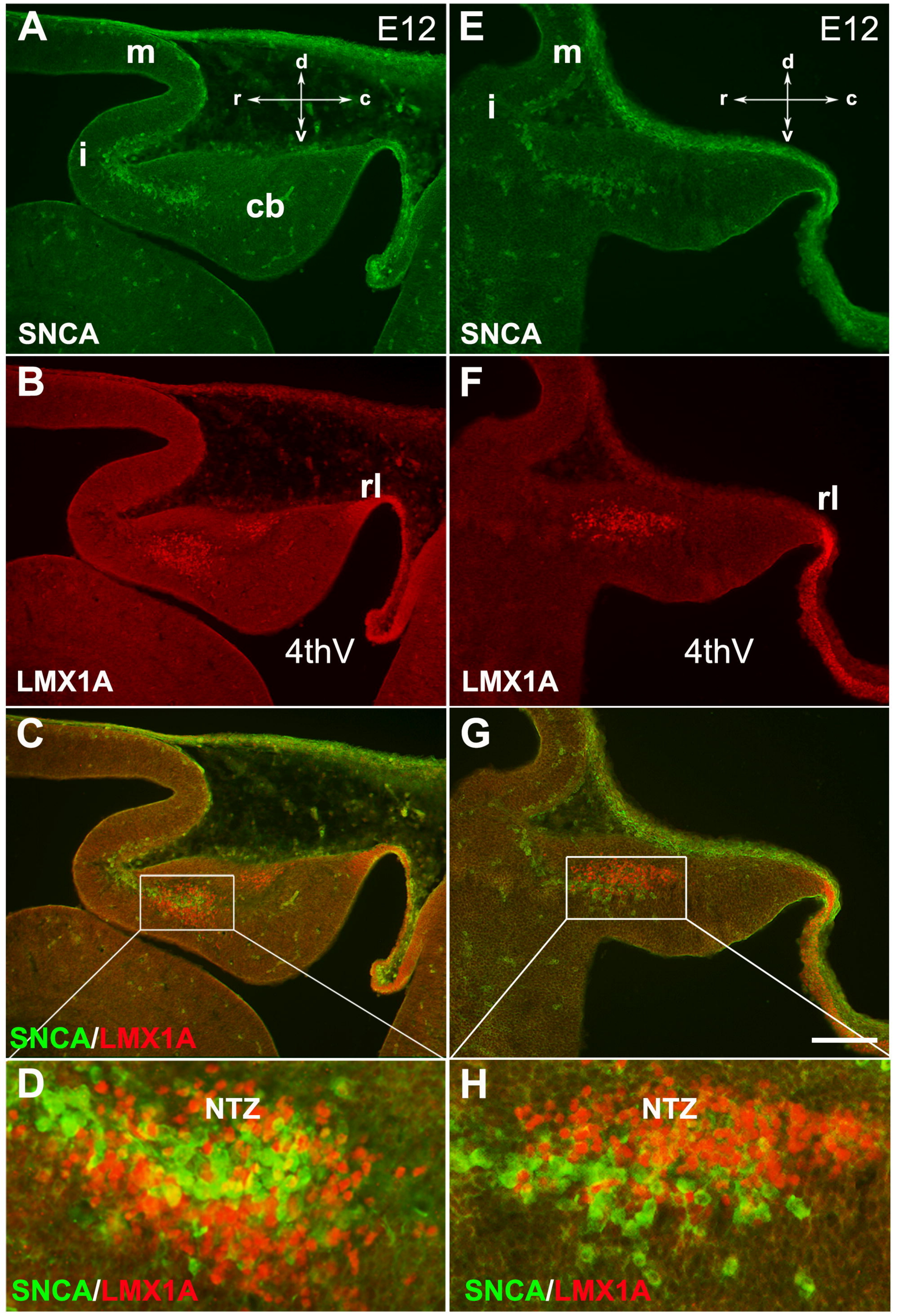
A
E12
m
d
r
c
v
i
cb
SNCA
E
E12
m
d
r
c
v
i
SNCA
B
rl
4thV
LMX1A
F
rl
4thV
LMX1A
C
SNCA/LMX1A
G
D
NTZ
SNCA/LMX1A
H
NTZ
SNCA/LMX1A

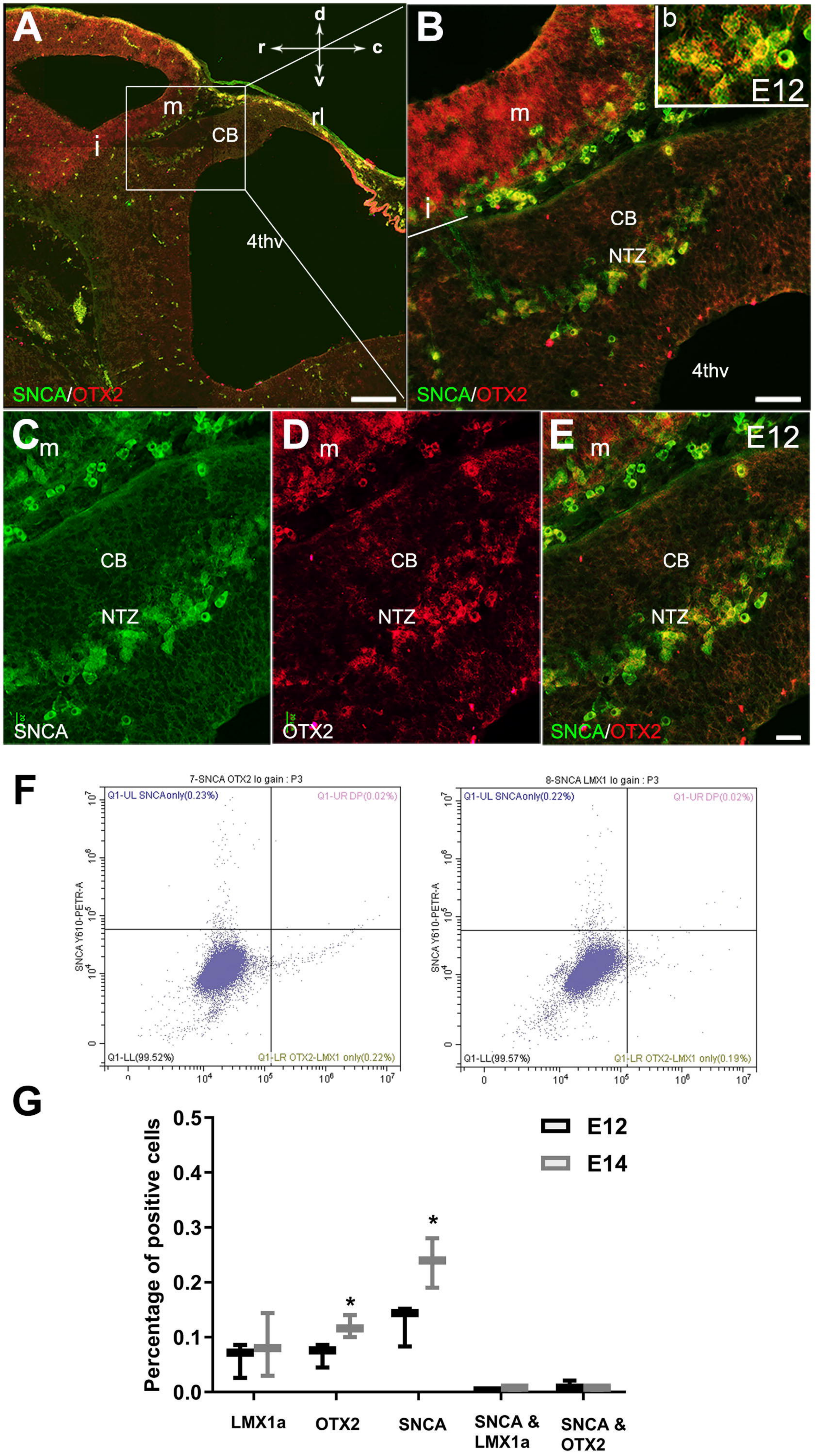
A
d
r
c
v
m
rl
CB
i
4thv
SNCA/OTX2
B
b
E12
m
i
CB
NTZ
4thv
SNCA/OTX2
C m
CB
NTZ
SNCA
D m
CB
NTZ
OTX2
E m
E12
CB
NTZ
SNCA/OTX2
F
7-SNCA OTX2 lo gain : P3
Q1-UL SNCAonly(0.23%)
Q1-UR DP(0.02%)
Q1-LL(99.52%)
Q1-LR OTX2-LMX1 only(0.22%)
SNCA Y610-PETR-A
8-SNCA LMX1 lo gain : P3
Q1-UL SNCAonly(0.22%)
Q1-UR DP(0.02%)
Q1-LL(99.57%)
Q1-LR OTX2-LMX1 only(0.19%)
SNCA Y610-PETR-A
G
E12
E14
Percentage of positive cells
0.5
0.4
0.3
0.2
0.1
0.0
*
*
LMX1a
OTX2
SNCA
SNCA & LMX1a
SNCA & OTX2

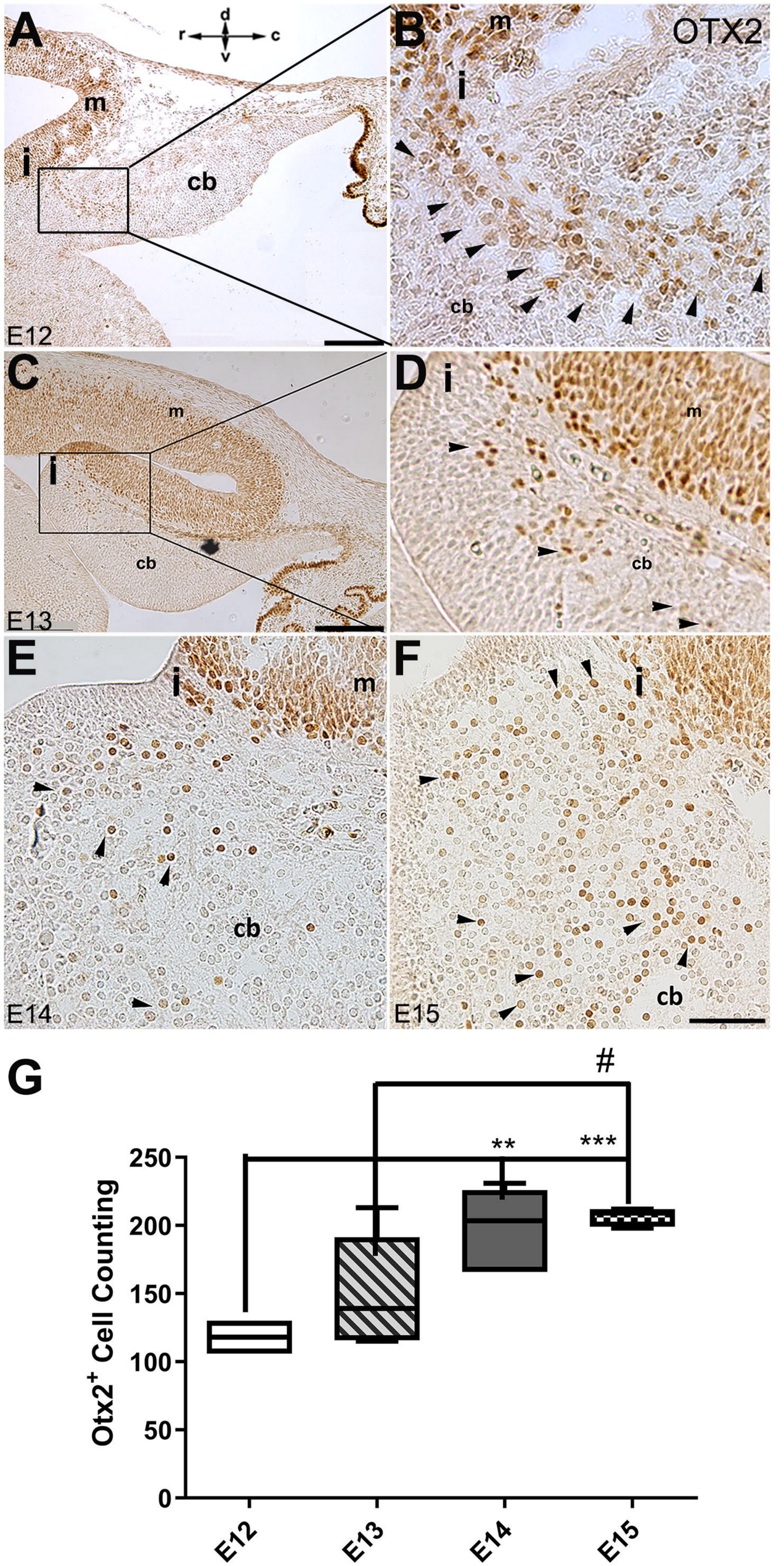
A
d
r
c
v
m
i
cb
E12
B
m
OTX2
i
cb
C
m
i
cb
E13
D
i
m
cb
E
i
m
cb
E14
F
i
cb
E15
G
#
**
***
250
200
150
100
50
0
Otx2+ Cell Counting
E12
E13
E14
E15

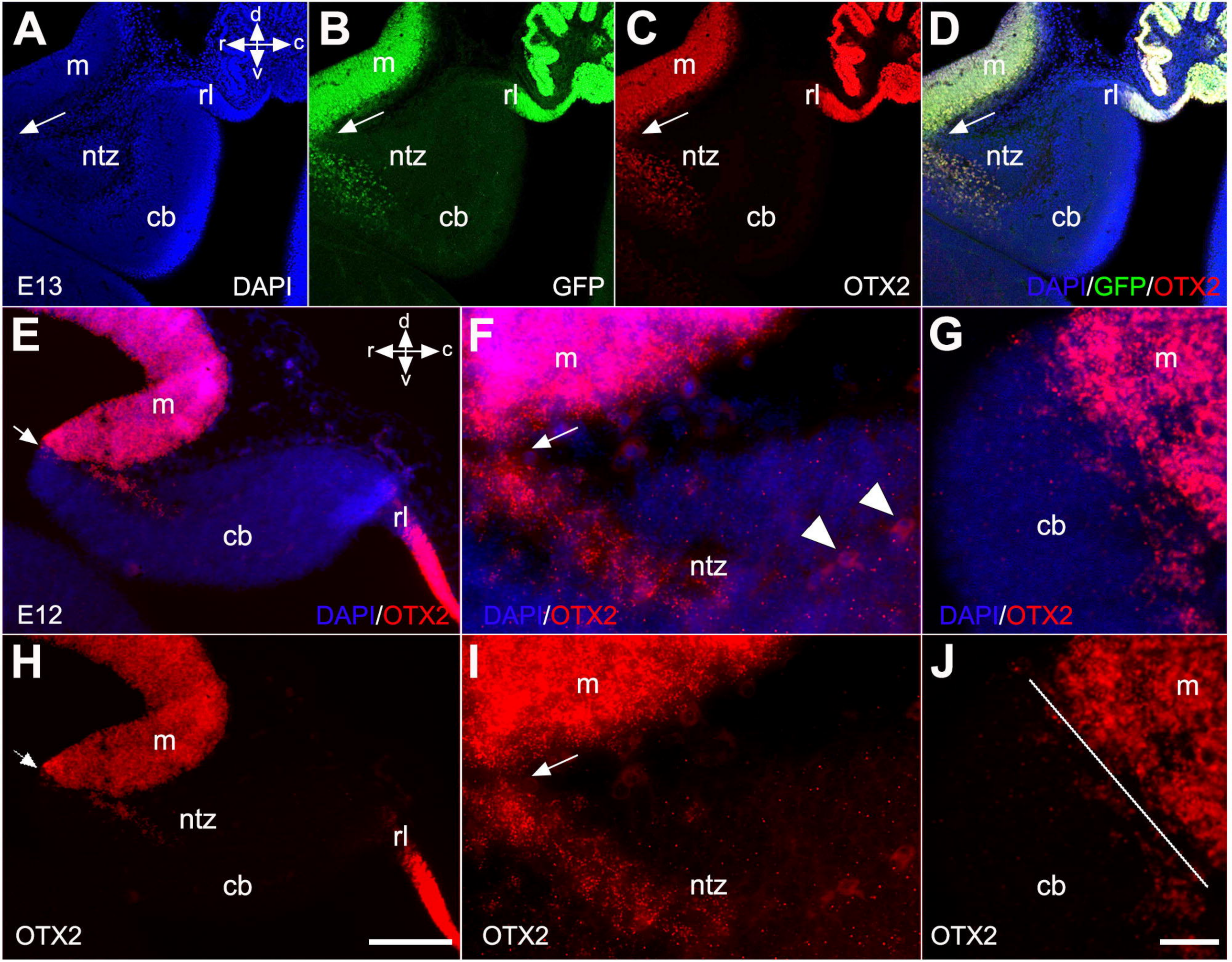
A
d
r
c
v
m
rl
ntz
cb
E13
DAPI
B
m
rl
ntz
cb
GFP
C
m
rl
ntz
cb
OTX2
D
m
rl
ntz
cb
DAPI/GFP/OTX2
E
d
r
c
v
m
cb
rl
E12
DAPI/OTX2
F
m
ntz
DAPI/OTX2
G
m
cb
DAPI/OTX2
H
m
ntz
rl
cb
OTX2
I
m
ntz
OTX2
J
m
cb
OTX2

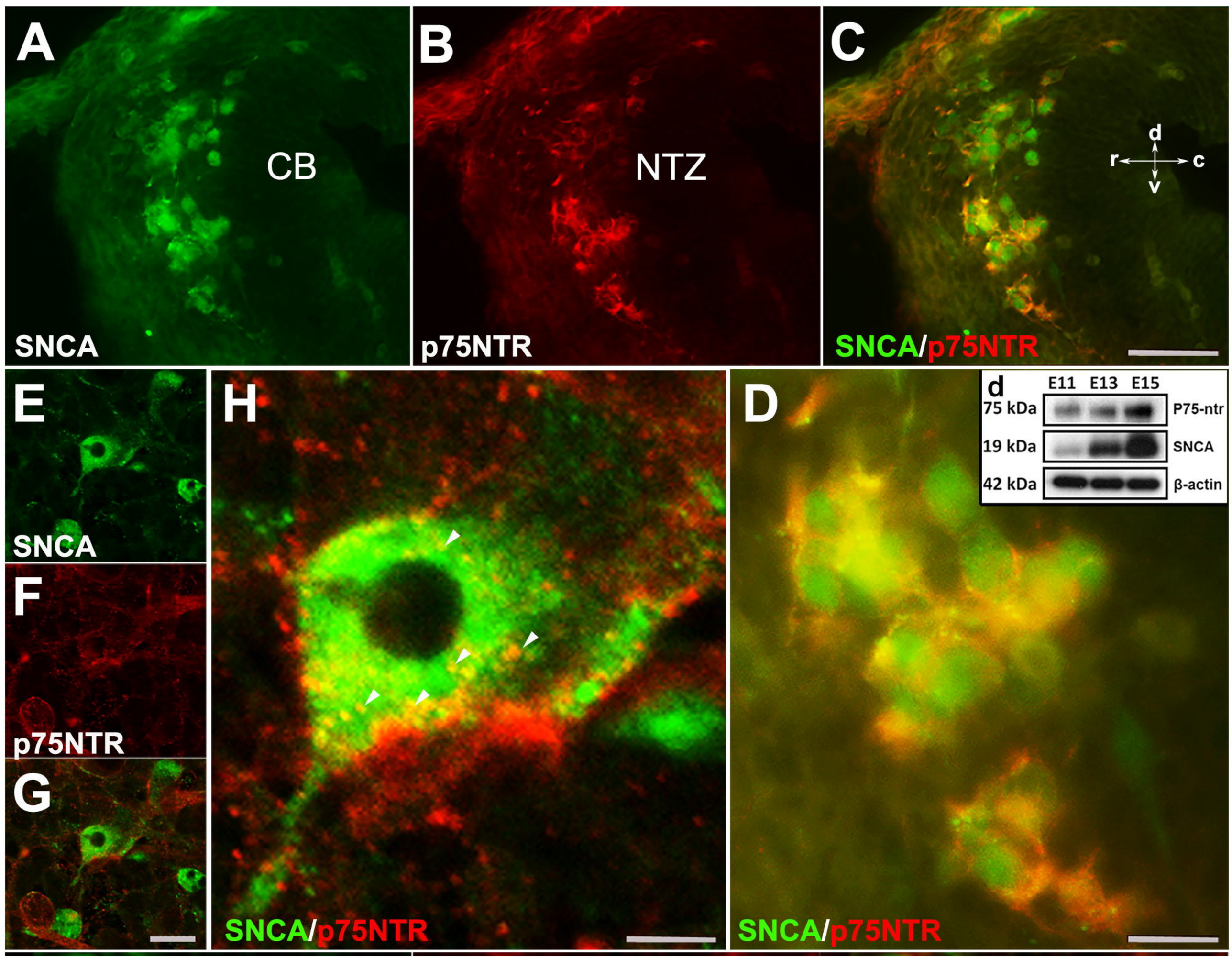
A
CB
SNCA
B
NTZ
p75NTR
C
d
r
c
v
SNCA/p75NTR
E
SNCA
F
p75NTR
G
H
SNCA/p75NTR
D
SNCA/p75NTR
d
E11 E13 E15
75 kDa
P75-ntr
19 kDa
SNCA
42 kDa
β-actin

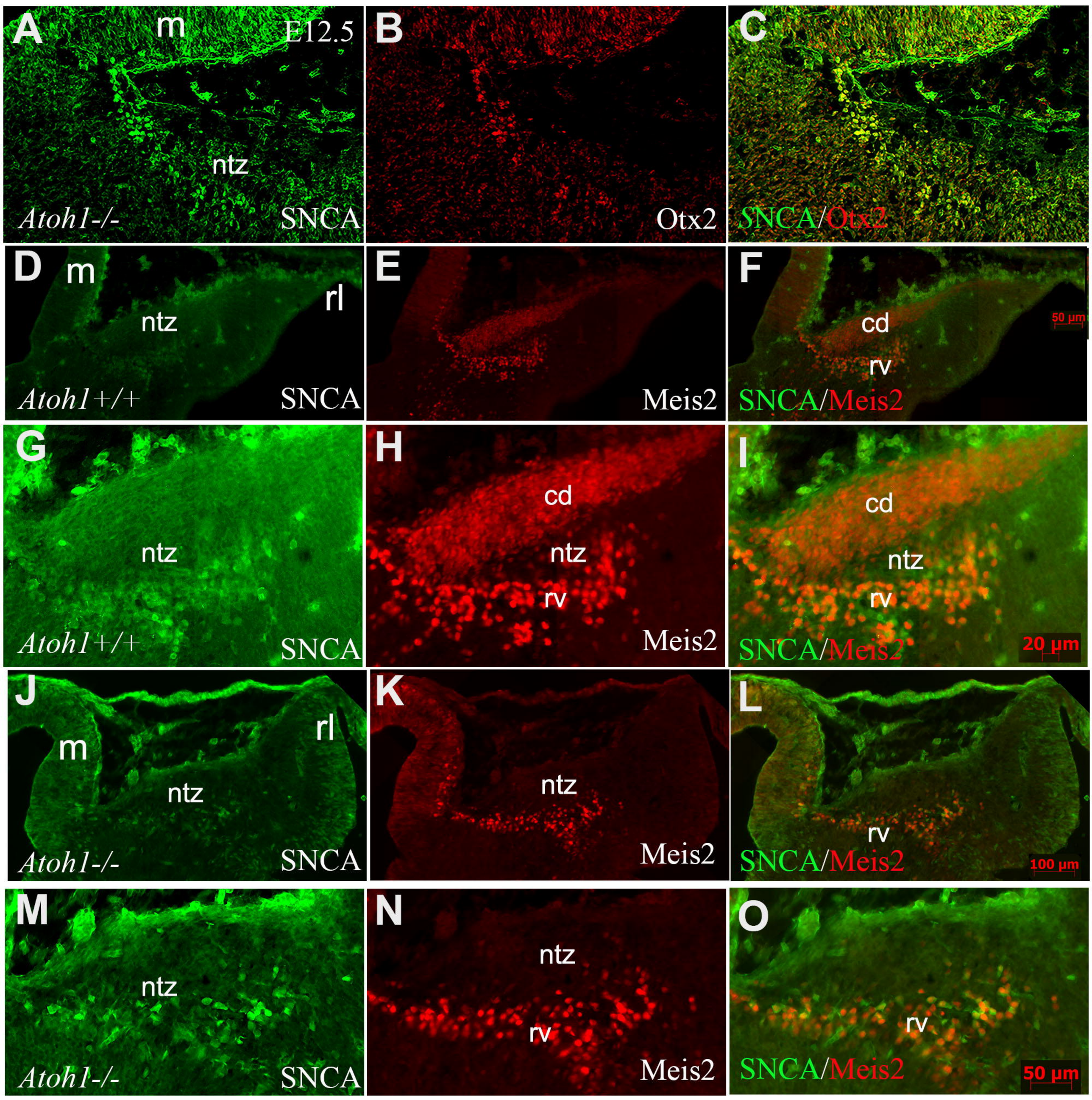
A
m
E12.5
ntz
Atoh1-/-
SNCA
B
Otx2
C
SNCA/Otx2
D
m
rl
ntz
Atoh1+/+
SNCA
E
Meis2
F
cd
rv
50 µm
SNCA/Meis2
G
ntz
Atoh1+/+
SNCA
H
cd
ntz
rv
Meis2
I
cd
ntz
rv
SNCA/Meis2
20 µm
J
m
rl
ntz
Atoh1-/-
SNCA
K
ntz
Meis2
L
rv
SNCA/Meis2
100 µm
M
ntz
Atoh1-/-
SNCA
N
ntz
rv
Meis2
O
rv
SNCA/Meis2
50 µm

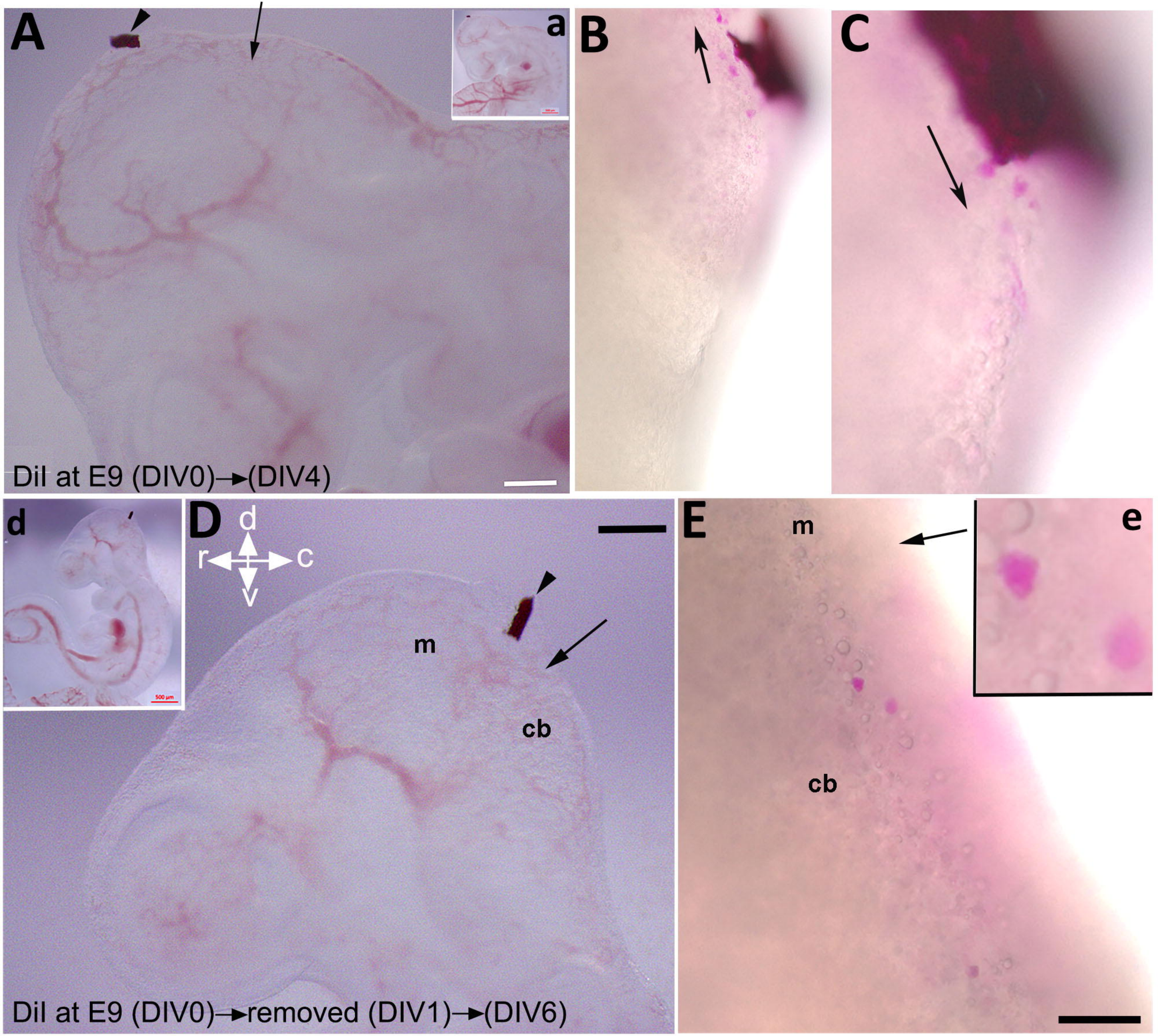
A
a
B
C
DiI at E9 (DIV0)→(DIV4)
d
D
d
r
c
v
m
cb
E
m
e
cb
DiI at E9 (DIV0)→removed (DIV1)→(DIV6)

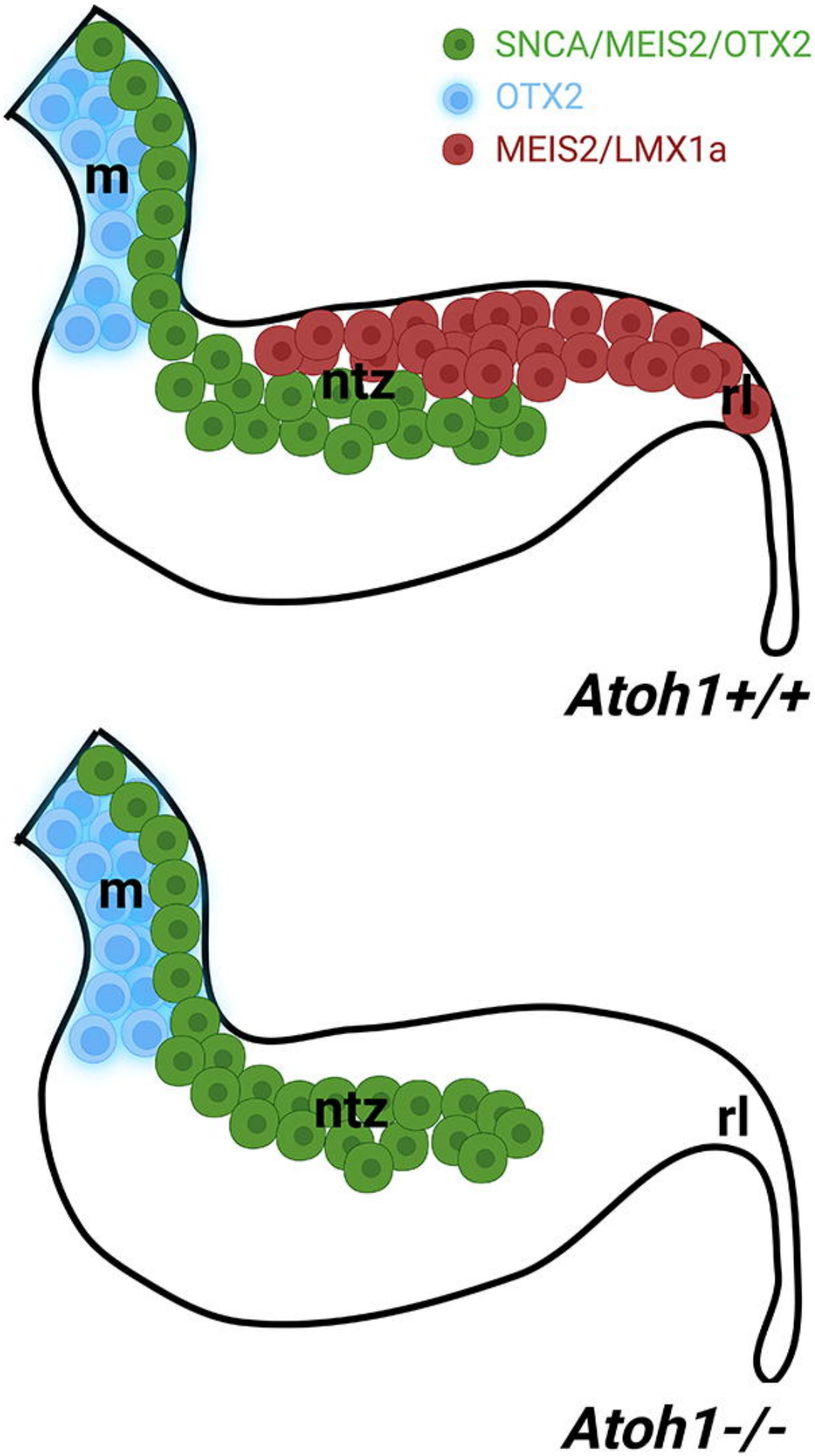
SNCA/MEIS2/OTX2
OTX2
MEIS2/LMX1a
m
ntz
rl
Atoh1+/+
m
ntz
rl
Atoh1-/-